ISSN 1392-1320 MATERIALS SCIENCE (MEDŽIAGOTYRA). Vol. XX, No. X. 2025

# Study on Wear Characteristics of Coal Drain Chute for Open Pit Mine

**Xuewei TAO [1, 2], Guoliang XIE [2], Mingxiang GUO [2], Zirun YANG [2], Yue HUANG [3] *, Runjie GONG [3]**

[1] *School of Safety Engineering, China University of Mining and Technology, Xuzhou, 221116, China*
[2] *Zhonglian Runshi Xinjiang Coal Industry Co. Changji, 831800, China*
[3] *School of Energy and Mining Engineering, China University of Mining and Technology, Beijing, 100083, China*

http://doi.org/10.5755/j02.ms.38746

*Received 9 September 2024; accepted 2 December 2024*

With the advancement of social science and technology and the escalating demand for resources, the utilization rate and load of mechanical equipment in diverse industries have become increasingly prominent. Mechanical malfunctions occur frequently, especially in material transportation, causing substantial economic losses. Mechanical wear has emerged as the principal cause of mechanical equipment failure; hence, studying the wear of particles and transportation machinery is of paramount importance. This paper utilizes the discrete element method and numerical simulation approach to investigate the influence of mechanical structure alterations on the wear of discharge chutes in coal conveyor systems. The results reveal that in terms of speed, reducing the conveyor belt speed has negligible effects on the falling trajectory and distribution characteristics of the materials but reduces the frequency of contact between the materials and the chute surface, thereby diminishing the tangential force exerted by the materials on the chute. The tangential cumulative force plays a crucial role in the wear of the chute by granular particles and can effectively alleviate the wear of the chute. With respect to the inclination angle of the conveyor belt, when increasing the angle clockwise, the influence on the falling trajectory and distribution characteristics is relatively minor, and the falling speed of the materials will accelerate. Nevertheless, the wear of the chute will decrease as the inclination angle increases. When increasing the inclination angle counterclockwise, the falling trajectory and distribution characteristics are significantly affected, and the materials will tend to concentrate, and the falling speed will decelerate, resulting in a substantial reduction in chute wear. These discoveries provide theoretical underpinnings for reducing equipment wear and optimizing coal transportation equipment.
*Keywords:* wear, EDEM, chute wear, simulation, abrasion resistance.

## 1. INTRODUCTION

As social science and technology advance, the widespread use of machinery and equipment has become increasingly common across all sectors. However, due to rising resource demands, machinery and equipment are experiencing heavier workloads, resulting in frequent mechanical malfunctions. The primary type of failure in the coal conveying system is wear failure, which significantly impacts production efficiency and poses a threat to the safety of workers' lives and property. Research indicates that 82 % of wear during mining operations involves surface damage to transportation equipment caused by materials such as coal [1]. The coal mining transportation system heavily relies on mechanical equipment, with the silo discharging chute being a key component [2]. The effectiveness of the chute significantly impacts the dependability and longevity of the system. In our research, the GOST 30479-97 standard, titled “Assurance of Wear Resistance in Products” plays a crucial role as it outlines essential requirements and testing methods for assessing the wear resistance of various products, especially those used in coal transportation systems. Adhering to this standard is critical for minimizing machinery failure rates and improving the durability of vital components like chutes and conveyors. The GOST 30479-97 provides a thorough framework for measuring the wear resistance of materials and structures, which is directly relevant to our study on the wear characteristics of coal drain chutes in open-pit mining operations. During the transportation of coal, there is a notable interplay between the coal and the chute, giving rise to the abrasion and deterioration of the chute [3 – 5]. As the materials travel through the lower section of the chute, prolonged wear and tear will hasten equipment damage and reduce its operational lifespan [6]. Hence, it is essential to examine the erosion scenario involving granular materials and chutes to assess the effectiveness of machinery and processing equipment. The existing literature often overlooks the potential impacts of belt speed and angle adjustments on wear traits during coal transportation simulations. This study addresses this gap by combining field experiments with discrete element method (DEM) simulations to provide a thorough understanding of the chute wear mechanism in coal transport systems. Our approach takes into account not only the material's physical properties but also how operational parameters influence the wear process, thus offering a fresh perspective on chute design and operation.

Abrasive wear is the degradation of material quality due to the interaction between resilient particles and the surface, leading to micro-cutting, formation of wedges, and ploughing on the material surface [0, 8]. Wear types can be classified into two-body and three-body categories, with three-body wear being the more prevalent [9]. In the abrasive wear research, Bialobrzeska et al. observed that in

* Corresponding author. Tel.: +8613288154813.
E-mail: *zqt2200101022@student.cumtb.edu.cn* (Y. Huang)

the grinding wheel wear test process, the wear behavior of boron steel is mainly caused by micro-cutting and micro-excavation., with the removal of larger particles resulting in visible wear patterns on the surface [10]. During the experiments involving wear tests on both the dry abrasive wheel, Nahvi et al. observed a correlation between the movement state of abrasive grains and factors such as shape, size, and speed when wear occurs [11]. Xu and colleagues examined of the wear conditions for various high-speed steels and determined that the dimensions of wear particles and the impact of the applied force significantly affected the high-speed steels' wear properties [12]. Woldman and colleagues studied how particle size, feed rate, and hardness affect wear [13]. When using the sand semi-free wear tester, it was observed that wear became more pronounced as pressure and sliding speed increased, but decreased as the proportion of water, coal, and gangue increased [14].

The Discrete Element Method (DEM) is a highly effective analytical tool, widely and effectively used to address discrete element issues due to its inherent characteristics [15]. The DEM model shows significant advantages when examining and assessing the minor interactions of particles in contact with processing and transportation equipment surfaces. Katterfeld et al. validated the impact plate transfer station of a high-capacity belt conveyor and assessed the influence of bulk materials on both the impact plate and the receiving belt conveyor [16]. Hastie and Wypych combined the discrete element method (DEM) with continuum theory to demonstrate their capability to accurately forecast the particle velocity distribution in bulk materials [17]. Jafari et al. utilized the Discrete Element Method (DEM) to explore how grid inclination, oscillation rate, and stimulation direction impact the wear. They noted a rise in the rate of wear with an rise in both vibration frequencies [18]. Professor Chen and colleagues utilized the Discrete Element Method (DEM) to incorporate a wear model into their investigation of single particle sliding wear [19]. L. Zhou et al. created a simulation-based abrasive jet test to accurately forecast the wear patterns of different materials when subjected to varying impact conditions [20].

In conclusion, the existing research level on the erosion wear of coal troughs is inadequate. Conventional wear tests do not accurately replicate real-world conditions. The test did not monitor the movement path of standard coal particles, nor did it analyze the breakage of these particles or measure the force between coal and chute. As a result, there was inadequate investigation into chute erosion caused by interactions among coal particles. This study integrates field experiments and simulations to investigate the wear of scraper conveyors. The field particle size is small and does not easily break into smaller particles. It is hypothesized in this study that the particles are rigid and directly impact the chute. Through this method, we preliminarily verify the calculated wear mechanism and evaluate the influence of adaptive environmental parameters using DEM to simulate particle collisions on a vertical chute. This study examines erosion caused by coal trough interaction under various conditions through simulation methods. The findings align with those of prior research, especially regarding the wear mechanism. It was observed that the speed and force of contact between the material and the chute have a substantial impact on chute wear, which differs from Bialobrzeska et al.'s [10] assertion that the primary factors influencing chute wear behavior are micro-cutting and micro-plow effects. The study suggests that adjusting conveyor belt speed and chute angle can effectively minimize chute wear. The discovery that cumulative tangential forces directly influence wear challenges certain assumptions made in previous studies about the relationship between material velocity, chute angle, and wear. The research results provide theoretical support for optimizing coal transportation equipment and offer a new theoretical perspective for reducing equipment wear.

## 2. DEM MODEL IMPLEMENTATION AND THEORY

The Discrete Element Method (DEM) is a computational technique that utilizes time integration to calculate the trajectory and rotation of individual particles within a specified domain using small time increments. This study adopts the discrete element method (DEM) in combination with numerical simulation techniques to explore the wear traits of coal bunker chutes. To ensure the lucidity and replicability of our results, we made use of EDEM version 2022 for our simulations. EDEM is a specialized commercial software customized for simulating granular materials, presenting advanced particle interaction models that incorporate normal and tangential contact as well as sliding interactions. In performing our simulations, we determined several crucial parameters: a time step of 0.01 seconds was fixed to guarantee accuracy; the friction coefficient between particles was specified at 0.5, with static friction at 0.36 and rolling friction at 0.05 – these values are founded on experimental outcomes and literature propositions. Furthermore, we utilized the Hertz-Mindlin contact model to portray elastic interactions among particles and implemented the Archard wear model to assess the surface wear degrees.

In this research, a model for soft coal particles was developed to simplify the discrete element method (DEM) model and enhance its capacity for validating experimental data. Currently, the soft particle method is the most prevalent technique, which accommodates multiple particle contacts, permits milder interactions, consequently diminishing computation time, and broadens the system's modeling range to encompass larger and more intricate scenarios [21].

### 2.1. Model for particle contact in discrete element systems

Soft-sphere model permits the crossing of components at contact points, and particle collisions can have a limited duration [22]. When loose coal is being transported by a scraper conveyor, the speed is not high, and there are simultaneous interactions among multiple particles. As a result, the soft ball contact model can be utilized. The representation of the softball model can be observed in the illustration (Fig. 1). When particle i contact with particle j at point C due to an external force or inertia. The initial position of the particle is indicated by a dashed line. As the objects move relatively, the particles deform and generate forces when they come into contact. The soft ball model

fails to adequately delve into the aspects of deformation; it specifically calculates tangential δ displacement and normal αoverlap to determine the force of contact.

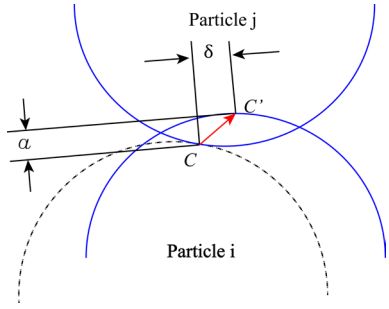


**Fig. 1.** Soft sphere particle model

The model establishes a connection between two particles by using a connecting device, elastic component, vibration absorber, and movable element. A coupler is employed to establish the association between the particles in proximity without the application of external force. Parameters are essential for characterizing the behavior of the spring, damper, and slider within soft sphere models. The interaction forces between particles constitute a theory of a fundamental aspect of soft sphere contact theory; categorizing the force into normal and tangential (refer to Fig. 2).

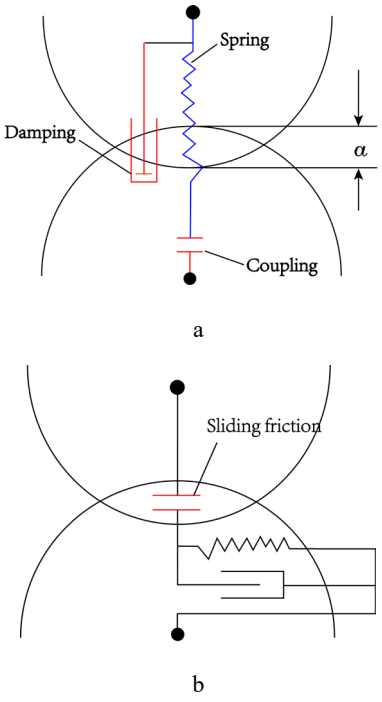


**Fig. 2.** The particles' interaction forces: a – normal stress; b – shear stress

The $F_{nij}$ is the normal force and the elastic force and damping forces that act on the particle. In the Hertz contact theory, $F_{nij}$ can be calculated in this manner:

$$F_{nij} = \left(-k_n a^{\frac{3}{2}} - c_n v_{ij} \bullet n\right) n. \quad (1)$$

The representation of the tangential force for $F_{tij}$:

$$F_{tij} = -k_t \delta - c_t v_{ct}, \quad (2)$$

where $n$ represents a unit vector that points from the center of particle i to the center of particle j; $\alpha$ represents the distance of overlap of normal orientation; $v_{ij}$ denotes particle i's the relative speed vector with respect to particle j; $\delta$ signifies tangential relocation at the contact; $k_n$ and $k_t$ are coefficients related to elasticity; $c_n$ and $c_t$ are coefficients associated with damping; and vct denotes the velocity of motion at the point of contact. Particle i's total force when in contact with multiple particles can be determined using a specific equation:

$$F_i = \sum_j (F_{nij} + F_{tij}). \quad (3)$$

The soft ball model's elasticity and damping coefficients have a direct correlation with the particles' elastic modulus and Poisson's ratio, typically necessitating calibration through experimental means. The normal elastic coefficient $k_n$ is based on the Hertz contact theory:

$$k_n = \frac{4}{3}\left(\frac{1-v_i^2}{E_i} + \frac{1-v_j^2}{E_j}\right)^{-1}\left(\frac{R_i+R_j}{R_i R_j}\right)^{-1/2}. \quad (4)$$

The elastic modulus of particle material is represented by $E$, while the Poisson's ratio of particle material is represented by $v$.

If the sphere is composed of identical materials and possess as equivalent radii, then $k_n$ can be simplified as follows:

$$k_n = \frac{\sqrt{2R}E}{3(1-v^2)}. \quad (5)$$

Determine the tangential elastic coefficient $k_t$ by utilizing the formula provided below:

$$k_t = 8\alpha^{1/2}\left(\frac{1-v_i^2}{G_i} + \frac{1-v_j^2}{G_j}\right)^{-1}\left(\frac{R_i+R_j}{R_i R_j}\right)^{-1/2}, \quad (6)$$

where the shear modulus is $G$.

If the sphere is made of the same material and has equal radii, then $k_t$ is:

$$k_t = \frac{2\sqrt{2R}G}{(1-v^2)}\alpha^{1/2}. \quad (7)$$

The tangential damping $c_t$ and normal damping $c_n$ are computed using the equations provided below:

$$c_n = 2\sqrt{m k_n}; \quad (8)$$

$$c_t = 2\sqrt{m k_t}. \quad (9)$$

During the contact process, it is necessary to compute the elastic coefficients associated with normal overlap in real-time. However, this computation places a significant load on the system. As a solution, the soft sphere model commonly assumes that both the elastic and damping coefficients stay constant during the entire contact procedure, without considering specific deformation and loading history.

## 2.2. Model for particle interaction

In the investigation, the interaction for particles of coal was established as the Hertz-Mindlin model with the assumption of no-slip condition. Particular models have demonstrated their precision and effectiveness in the computation of particle interaction and impact. It is

postulated that when spherical particles with $R_1$ and $R_2$ come into elastic contact, the normal force $F_n$ between them can be determined using the subsequent equation.

$$F_n = \frac{4}{3}E^*(R^*)^{1/2}\alpha^{3/2}. \quad (10)$$

The elastic modulus $E^*$ that is equivalent is result of dividing the equivalent radius $R^*$ by the normal overlap. The normal damping force $F_{nd}$:

$$F_n^d = -2\sqrt{\frac{5}{6}}\beta\sqrt{S_n m^*}v_n^{rel}. \quad (11)$$

The equivalent mass $m^*$ is determined by the product of the normal direction stiffness Sn and the $v_n^{rel}$ is the normal relative velocity.

The particles' tangential force compute using this formula:

$$F_t = -S_t\delta, \quad (12)$$

where $S_t$ represents the stiffness in the tangential direction; $\delta$ denotes the overlap in the tangential direction.

The tangential damping force $F_t$ between particles can be computed by this equation:

$$F_t = -2\sqrt{\frac{5}{6}}\beta\sqrt{S_t m^*}v_t^{rel}, \quad (13)$$

where $v_t^{rel}$ is tangential relative velocity. Friction is a function of the static friction coefficient $u_s$ and the force $F_n$.

Furthermore, it is essential for the simulation to consider the implications of rolling friction, which links to the torque $T_i$.

$$T_i = -u_r F_n R_i \omega_i, \quad (14)$$

where $R_i$ symbolizes the distance between the center of mass and the point of contact; $\mu_r$ is used to indicate the rolling friction coefficient; $\omega_i$ stands for the unit angular velocity vector at the contact.

## 2.3. Wear model

In industrial production, machinery is exposed to a variety of wear and tear challenges. Wear denotes the decrease in the geometric volume of components, resulting in part malfunction, reduced precision in machine operation, shortened lifespan of the machine system, or even complete loss of functionality for the parts. By implementing more deliberate design and conducting comprehensive research on wear, its impact can be mitigated. Wear can be classified into adhesive, particle, fatigue, and corrosion types based on different mechanisms. In practical applications, multiple mechanisms typically coexist simultaneously; however one type often assumes a dominant role. For example, during material transfer processes where materials continuously collide and rub against chutes while taking into account factors such as relative speed and impact angle. The wear described in this article primarily stems from the combined effect of impact and particle rolling within the chute. The particle type mainly presents itself in two forms: triad type caused by free particles moving between two friction surfaces; and biad type caused by particle contact with fixed solids during relative movement. Fig. 3 shows the mechanism of abrwear.

The expanded Archard wear model is well-suited for this type of wear mechanism since the depth of wear is directly proportional to the distance of friction, normal load, and wear coefficient, while being inversely proportional to the hardness of the material. EDEM includes an integrated Archard wear model based on Hertzian and Middlin-Deresiewicz contact theories, which was utilized in this study alongside the Hertz-Mindlin model and Archard wear model.

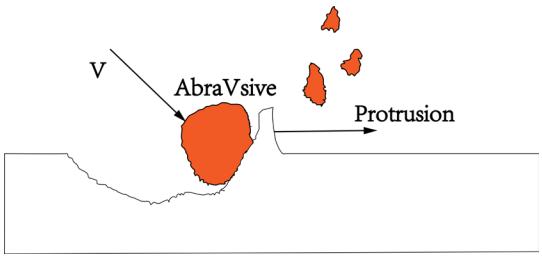


**Fig. 3.** Wear schematic diagram

As per the model, the volume of wear $V$ is:

$$V = K\frac{NL}{H}. \quad (15)$$

The normal load, wear coefficient ($K$), sliding distance ($L$), and the hardness of the abrasive material (H) collectively determine the wear volume ($V$) of a plane.

$$W = K/H, \quad (16)$$

where $W$ represents the constant for wear, which is the parameter in EDEM, a software utilizing the DEM for simulating bulk material behavior, is utilized to express the failure volume $V$ of geometry as follows:

$$V = WNL. \quad (17)$$

Within the Archard model, determining the wear coefficient $K$ presents significant challenges due to its reliance on a variety of wear factors, including but not limited to hardness $H$, except the normal load and sliding distance. The role of hardness is paramount in influencing the frictional wear factor.

In the simulation software EDEM, the failure depth h of wear:

$$h = V/A, \quad (18)$$

where $A$ represents the acreage from which material has been extracted.

# 3. MODEL BUILDING

## 3.1. 3D geometric model of the coal transport system

This paper focuses on the coal transport system of the coal bunker at Zhonglian Runshi Company in the Xiheishan Mining Area of Xinjiang, with a simulation of the impact of bulk materials on the chute (as illustrated in Fig. 4). A simplified diagram of the on-site equipment is depicted in Fig. 5, which includes a coal feeder and a vertical chute. The material flows from the silo to the coal feeder via a conveyor belt, then enters the chute and precisely feeds into the coal car. The belt speed of the coal feeder is readily adjustable and obtainable. Throughout this process, there is consistent

impact and wear effect exerted by the material flow on the chute, where it continuously impacts from the conveyor belt onto the vertical chute. At the rear end of the conveyor belt lies a telescopic chute comprising two bushings made of similar material that can be freely extended. The simulation was developed using an accurate scale model of the open-pit mining production system, which guarantees both its precision and practical applicability.

**Fig. 4.** Coal transport system site diagram

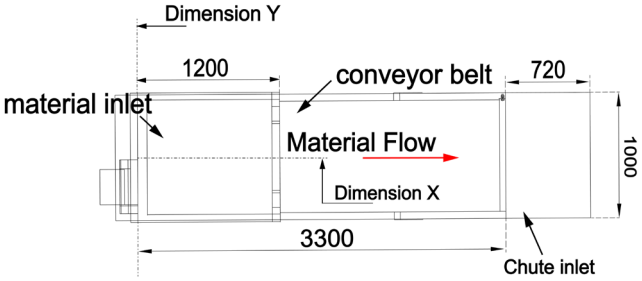


panel view

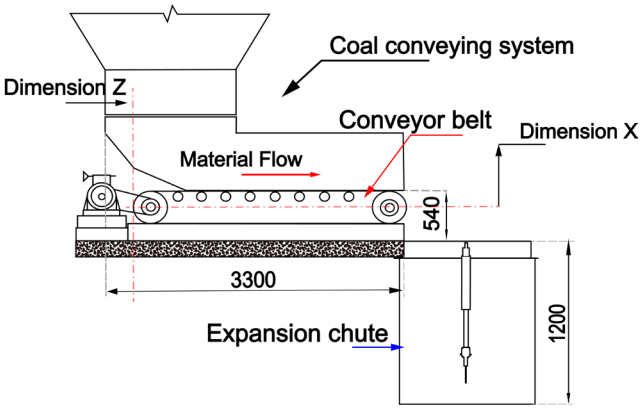


elevation view

**Fig. 5.** Simple schematic diagram of the coal transport system

While the coal conveying system is in operation, the abrasive nature of loose coal results in wear to the coal discharging chute. This study focuses solely on chute wear during the transmission process and selects coal from the conveyor as its primary research subject. In practical production, there is a high frequency of coal transportation, and most of the chute wear occurs when the chute is fully extended. Therefore, only wear under this fully extended state is taken into consideration, simplifying the model, as shown in Fig. 6. The wear simulation of the coal discharging chute determined the coal particles' total mass in close proximity to this actual situation, and the simulation time was 5 seconds. The wear between the particles and the chute begins as soon as they come into contact with the inner wall. To better replicate the actual steady flow state, when the particles are produced in the pellet plant, the same velocity is initially given to the coal conveyor, and the particles keep a linear movement along with the conveyor belt.

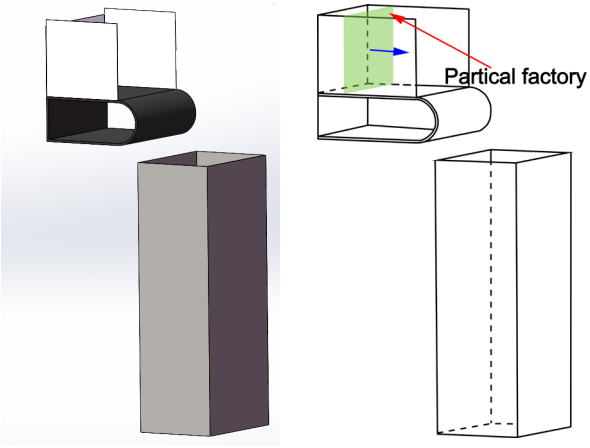


**Fig. 6.** Simple model of the coal conveying system

In the coal discharging chute, under gravity's influence, coal material is transported downward, and it is conveyed throughout this process.

## 3.2. Particle model

In this research, we established the typical dimensions and configurations of coal particles through a series of screening tests, as illustrated in Fig. 7. Initially, the findings from these experiments highlighted the distribution patterns of coal particles, enabling us to recognize two primary shapes that together formed the bulk of the coal flow. Given that these morphological characteristics significantly influence both the dynamic behavior and wear patterns during transport, we carefully considered them. The choice of particle shapes was influenced by discrete element simulation (DEM) requirements, which necessitated a reasonable simplification of coal particle geometries to maintain both accuracy and computational efficiency in our simulations.

**Fig. 7.** Screening experiment

With these considerations in mind, we identified representative sizes and shapes for coal particles, laying a robust groundwork for further investigation into their wear properties within chutes.

Indeed, the non-uniform nature of coal particles results in a wide range of shapes. EDEM can to simulate the morphology of coal particles by aggregating multiple small

spheres. The accuracy of the results is directly related to how closely the particle model resembles real particles. However, an excessive number of spheres can significantly impact computational efficiency. In this study on wear simulation, two different types of particle shapes (as depicted in Fig. 8) represent the fundamental forms of coal particles, with (a) tetrahedron particle representing 80% and (b) trigonal particle representing 20% of the total particle quantity. This research employs the coal particle with a diameter of 12 millimeters for wear simulation.

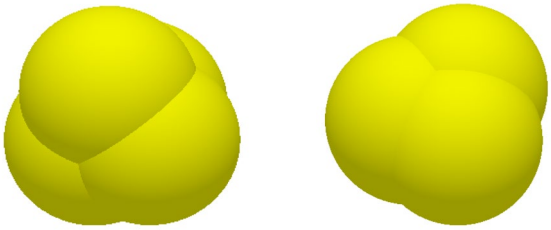

a b

**Fig. 8.** Graphic diagram of particles: a – tetrahedron particle; b – trigonal particle

### 3.3. Contact parameterization

During the process of simulating wear, the contact model employ the Hertz-Mindlin (no slip), and Archard wear and Relative Wear were chosen to replicate the interaction of structure and particles. Internal parameters were sourced from field material testing and configured according to the specifications in Table 1. Contact parameters were established as per the details provided in Table 2. The frictional wear constant between coal and steel is 8e-12 [23]. The simulation is configured with a time step that is 30 % of the time step used in Rayleigh's method. The simulation data is saved at intervals of 0.01 seconds.

**Table 1.** Intrinsic parameters

| Intrinsic parameters | Density, kg/m$^3$ | Poisson's ratio | Shear modulus, Pa |
|---|---|---|---|
| Coal | 1500 | 0.28 | 1.98e+7 |
| Steel | 7850 | 0.3 | 7.9e+10 |

**Table 2.** Contact parameters

| Contact parameters | Coefficient of restitution | Coefficient of static friction | Coefficient of rolling friction |
|---|---|---|---|
| Coal – Coal | 0.5 | 0.36 | 0.05 |
| Coal – Steel | 0.5 | 0.5 | 0.05 |

## 4. RESULTS AND ANALYSIS

This research focuses on examining the erosion characteristics of coal within a specific segment of the coal transportation system. The movement state, as depicted in Fig. 9, can be divided into three main sections. Initially, the lower coal is transported horizontally by the conveyor belt at an equivalent speed to that of the conveyor belt itself. Subsequently, it experiences parabolic motion with an initial velocity (as shown in Fig. 9 where speed can be broken down into horizontal $V_x$ and vertical $V_y$). At the junction of the conveyor belt and chute, there exists no horizontal gap but rather a vertical separation of 540 mm. The coal passes through the end of the conveyor belt with a consistent horizontal velocity while its vertical velocity increases due to gravitational acceleration g = 9.8 m/s$^2$; falling and impacting against the inner wall of the chute along the direction of the conveyor belt.

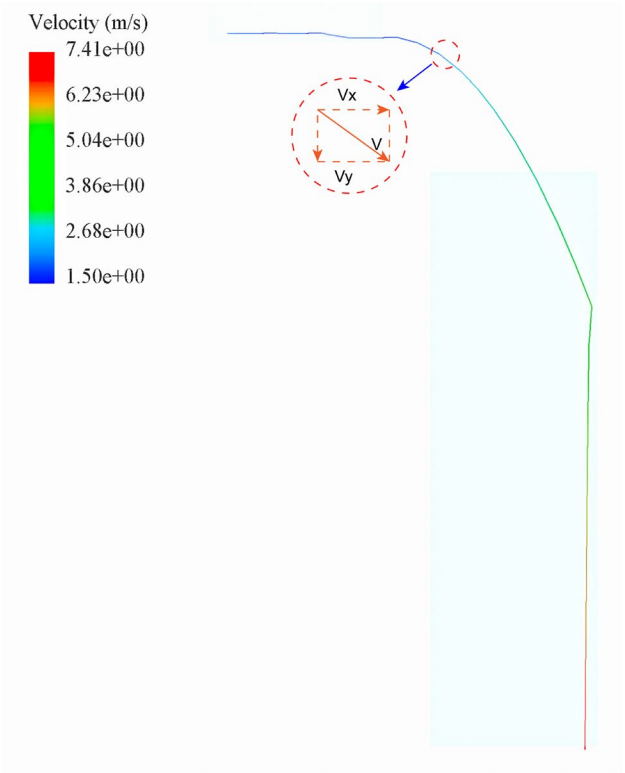


**Fig. 9.** Single particle movement trajectory

Finally, following impact against the inner wall of the chute, both horizontal and vertical velocities decrease simultaneously under force interactions and momentum conservation between elastic properties of both coal material and inner wall causing a change in direction before continuing parabolic motion at certain speeds with constant horizontal velocity but increasing the vertical velocity at certain speed due to gravitational acceleration $g$ when leaving chute; resulting in particle having maximum horizontal velocity $V_{xmax}$ and minimum vertical $V_{ymin}$ upon leaving belt; minimum horizontal velocity $V_{xmin}$ but greater than initial position $V_{ymin}$ upon collision with an inner wall; reaching maximum $V_{ymax}$ upon leaving the chute.

### 4.1. Experimental data and statistical analyses

In order to assess the influence of modifying the conveyor belt's speed and angle on reducing material wear in the chute, we conducted a series of experiments. Throughout these tests, we recorded data on chute wear at different conveyor belt speeds (0.5 m/s, 1 m/s, 1.5 m/s, 2 m/s) and angles (0°, 10°, 20°, 30°). The results indicate that at a conveyor belt speed of 0.5 m/s, the wear experienced by the chute is considerably less than under other speed conditions (Fig. 10). Furthermore, as the angle of the conveyor belt increases from 0° to 30°, there is a gradual reduction in abrasion; however, a notable decrease occurs when the angle reaches –30° (Fig. 13). These findings were statistically validated using one-way analysis of variance (ANOVA), confirming that both conveyor belt speed and angle significantly affect chute abrasion

($p < 0.05$), thereby reinforcing our conclusion.Specifically, we applied several statistical methods for data analysis:

Repeated measures ANOVA was employed to evaluate how varying speeds and angles impacted abrasion levels.The Tukey HSD post-hoc test was utilized to identify which specific groups showed significant differences.A significance threshold of 0.05 was established for all statistical evaluations. The outcomes from this statistical examination illustrate that adjustments in both conveyor belt speed and angle substantially influence chute wear, thus corroborating conclusions drawn from our simulations. These insights provide an experimental foundation for optimizing chute design within coal transport systems.

## 4.2. The impact of velocity on the erosion of the chute inner wall

The operation of coal transportation within the coal transport system leads to an acceleration in the velocity of coal particles as a result of gravitational forces. This, in turn, causes continuous high-speed impact and abrasion on the inner wall of the chute, resulting in wear, breakage, and potential fracture. The distribution pattern of impact load at varying conveyor belt speeds is depicted in Fig. 10. Based on the data presented in Fig. 10, when the belt speed is at 0.5 m/s, there is minimal impact of particulate material on the chute, resulting in decreased friction and a shallow wear depth (less than 2.7e-5mm). The wear tends to be concentrated in the lower section of the chute surface.

When the belt speed increases to 1 m/s, there is an observable rise in the influence of particulate material on the chute, leading to a wider range of wear with concentration towards the upper part of the chute surface. The wear depth remains below 3.7e-5 mm and primarily concentrates around the middle area. At a belt speed of 1.5 m/s, there is further escalation in impact from particulate material with an expanded but upwardly shifted wear range and concentration towards areas with increased wear depth (below 4.42e-5 mm), still predominantly focused around the middle region. Finally, at a belt speed of 2 m/s, there is a substantial increase in impact from particulate material resulting in reduced overall wear range but more pronounced concentration and upward shift. Wear depth remains below 4.87e-5 mm and continues to be concentrated primarily around the midsection.

The broadest wear distribution range is observed at the lowest level of wear when coal particles are loaded at a speed of 0.5 m/s, as depicted in Fig. 10. As the velocity increases to 2 m/s, there is a reduction in the impact range of coal particles on the chute. The upward shift in particle impact position due to an increase in belt speed results in a higher number of particles adhering to the chute surface for extended durations. This consequently leads to heightened static friction between the particles and the chute, causing an increase in friction distance and ultimately contributing to escalated chute wear. Furthermore, owing to the elevated belt speed, particles exhibit greater velocities ($V_{xmax}$,$V_y$) before impacting the chute, thereby intensifying erosion and chiseling effects on the chute and further exacerbating wear.

The results of the statistical simulation for conveyor velocity and cumulative force are displayed in Fig. 11, illustrating the correlation between (a) conveyor velocity and normal cumulative force, as well as (b) conveyor velocity and tangential cumulative force.

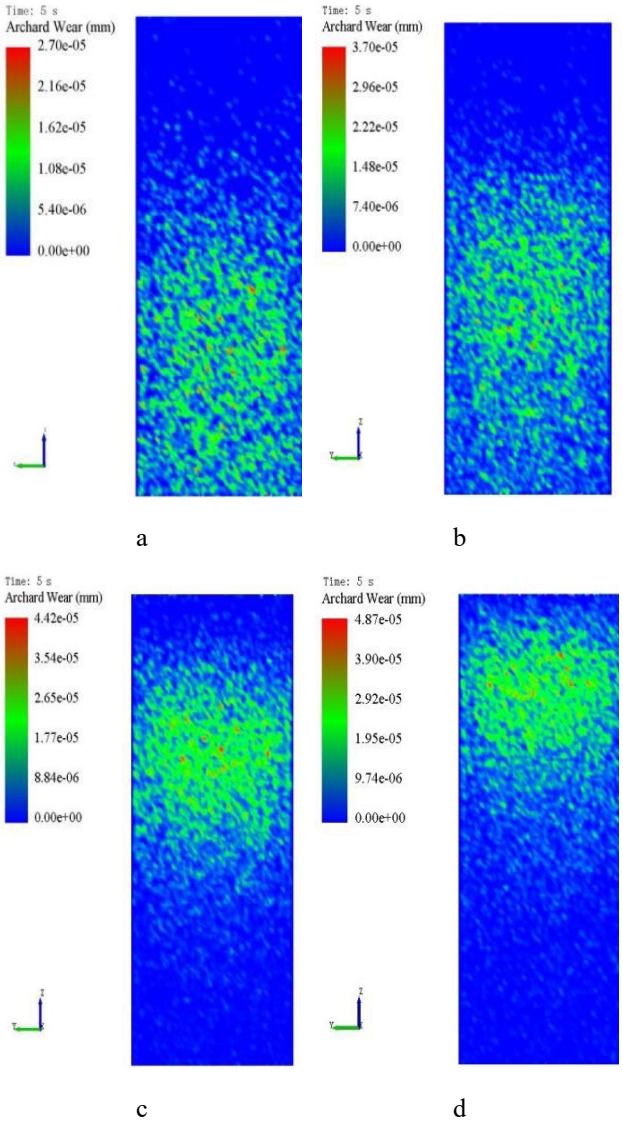


**Fig. 10.** At different conveyor belt speeds,where: a – 0.5 m/s; b – 1 m/s; c – = 1.5 m/s; d – = 2 m/s

As coal time increases, there is an observable upward trend in chute cumulative force. Specifically, at a chute velocity of 0.5 m/s, the normal cumulative force measures 1.48 N with a corresponding tangential value of 5.46 N; when the chute velocity reaches 1 m/s, the normal cumulative force rises to 2.10 N while the tangential cumulative force increases to 7.85 N; similarly, at a chute velocity of 1.5 m/s, we observe a normal cumulative force of 3.22 N alongside a tangential value of 12.55 N; finally, at a conveyor speed of 2 m /s ,the corresponding values are approximately 3.93 N for normalcumulativeforceand 14.15 N for tangential cumulative force.

The correlation between the cumulative normal force of chutes at varying conveyor speeds can be summarized as follows: 2 m/s > 1.5 m/s > 1 m/s > 0.5 m/s. This occurrence can be attributed to multiple factors. At a velocity of m/s, the coal impacts the inner wall directly due to its high speed and increased contact with the chute. Furthermore, particles exhibit a higher initial velocity and horizontal-oriented

component *V*x, resulting in elevated impact kinetic energy and subsequent normal accumulation force on the inner wall of the chute. Conversely, as the conveyor belt speed decreases, there is a reduction in impact kinetic energy which leads to a diminished effect on the inner wall and subsequently decreased normal accumulation force.

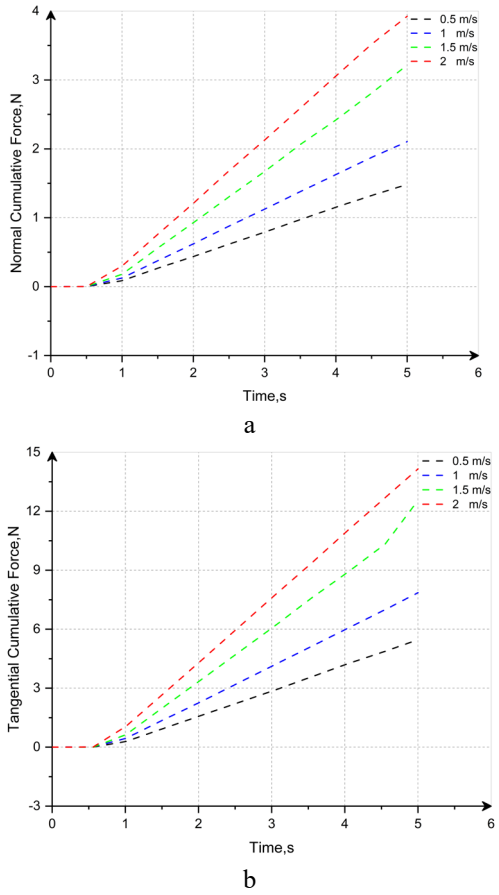


**Fig. 11.** Cumulative force and velocity of the chute

The tangential accumulation force of the inner wall of the chute changes in response to variations in conveyor belt speeds, exhibiting a trend where 2 m/s is greater than 1.5 m/s, which is greater than 1 m/s, and then 0.5 m/s. This phenomenon is impacted by several contributing factors. When operating at a speed of 2 m/s, coal makes contact with the chute wall from a more considerable distance, resulting in heightened damage to the wall and an increased tangential accumulation force. Conversely, as the conveyor speed decreases, the point of impact for the coal moves closer to the discharge port, ultimately leading to diminished damage on the inner wall and reduced tangential accumulation force. Fig. 12 illustrates the interaction between particles and the chute wall at various speeds from an alternative viewpoint. As the velocity reduces, the frequency of particle contact with the chute wall diminishes, thereby explaining the reduction in both the cumulative contact force and the wear rate as the speed decreases.

The comparison was made between the cumulative contact energy of the inner wall of the chute at four different conveyor belt speeds, indicating that the normal accumulation force and wear of the chute are minimized when operating at a speed of 0.5 m/s. The absence of normal cumulative contact energy in the inner wall of the chute during 0 ~ 0.5 s is due to coal not yet making contact with the chute; from 0.5 ~ 2 s, there is a steady increase in cumulative force. It can be observed that tangential cumulative force plays a significant role in chute wear. In summary, an increase in conveyor belt speed will worsen chute wear and reduce its service life.

Similar to the discoveries of H. Zhang et al.[24], our study confirms that tangential cumulative force is a critical factor in chute wear. However, our research expands on this understanding by quantifying the impact of conveyor belt speed on reducing wear, an aspect that has not been thoroughly explored in existing literature. By adjusting the conveyor belt speed, we effectively reduced the tangential force exerted by the material on the chute, aligning with the principles of contact mechanics as explained by M.A. Moore [**Error! Reference source not found.**].

### 4.3. The angle of the influence of the chute wall wear

The impact of varying conveyor belt angles on the state of particle movement is illustrated in Fig. 13, with a conveyor belt speed of 2 m/s and a load of 250 kg at t = 5 s.

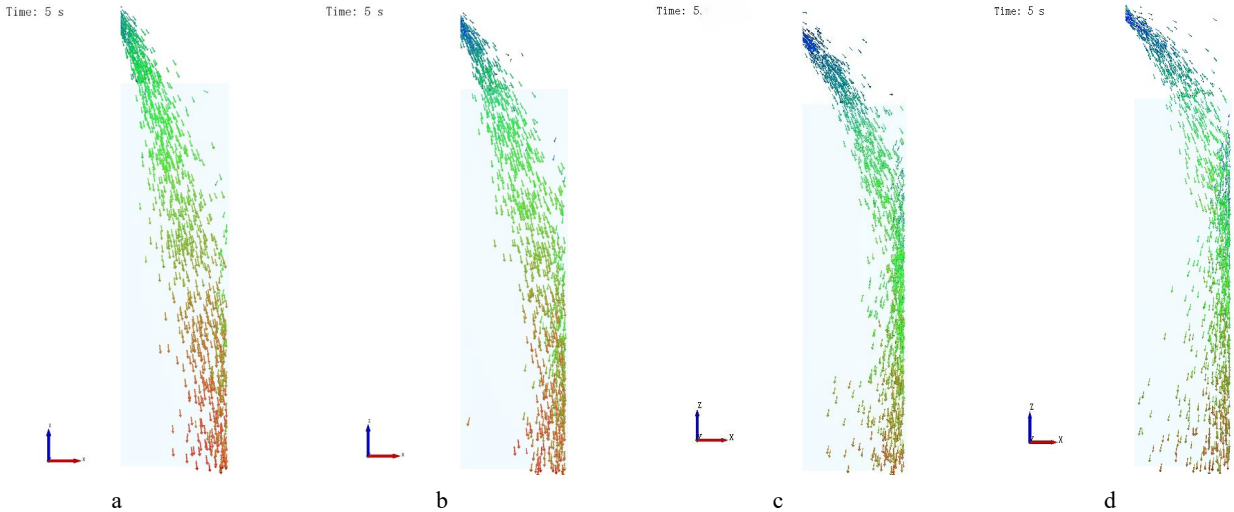


**Fig. 12.** Diagram of particle movement in the chute at different conveyor belt speeds: a – 0.5m/s; b – 1m/s; c – 1.5m/s; d – 2m/s

It can be observed from the figure that changes in the angle of the conveyor belt have a significant effect on particle movement. In the range of 10° to 30°, as the angle decreases, particles collide with the inner wall, resulting in reduced contact between some coal particles and the chute's inner wall.

Based on the data presented in Fig 14, alterations in the angle of the conveyor belt have a significant impact on particle velocity. As depicted in Fig. 14 a, when the conveyor belt angle varies from 10 to 30 degrees, there is a notable increase in particle velocity compared to an angle of 0 degrees. However, within this range, there is no discernible effect on particle velocity. Throughout the process of coal transfer, there is a consistent linear growth in particle velocity. In Fig. 14 b, as the conveyor belt angles range from –10 to –30 degrees, overall particle velocity decreases with the change in angle. Initially, there is a decrease followed by linear growth; however, ultimately resulting in lower final velocities than those observed at an angle of 0 degrees. According to the analysis conducted in Fig. 13, variations in angle can impact both particle velocity and impact position on the chute surface which subsequently influences wear patterns on the chute itself.

The angle of the conveyor belt, as shown in Fig. 15, varies from 0 to 30 degrees, resulting in a significant decrease in chute wear. However, there is relatively little change in the impact position on the chute. Simulation' results presented in Fig. 12, Fig. 13, and Fig. 14 a indicate that with an increase in the conveyor belt angle from 0 to 30 degrees, there is a rise in particle contact with the inner wall of the chute. This offsets the reduction in contact mass and ultimately reduces chute wear up to a specific value.

As the angle of the conveyor belt shifts from 0 to –30, it is apparent from Fig. 16 that there is a notable decrease in the wear amount of the chute as the angle decreases, and the impact position of particles on the chute gradually shifts downward. When considering the simulation results presented in Fig. 12, Fig. 13, and Fig. 14 b, it becomes evident that an increase in conveyor belt angle from 0 to 30 results in a reduction in contact quality between the inner wall of particles and chute, consequently leading to a decrease in wear value of the conveyor belt.

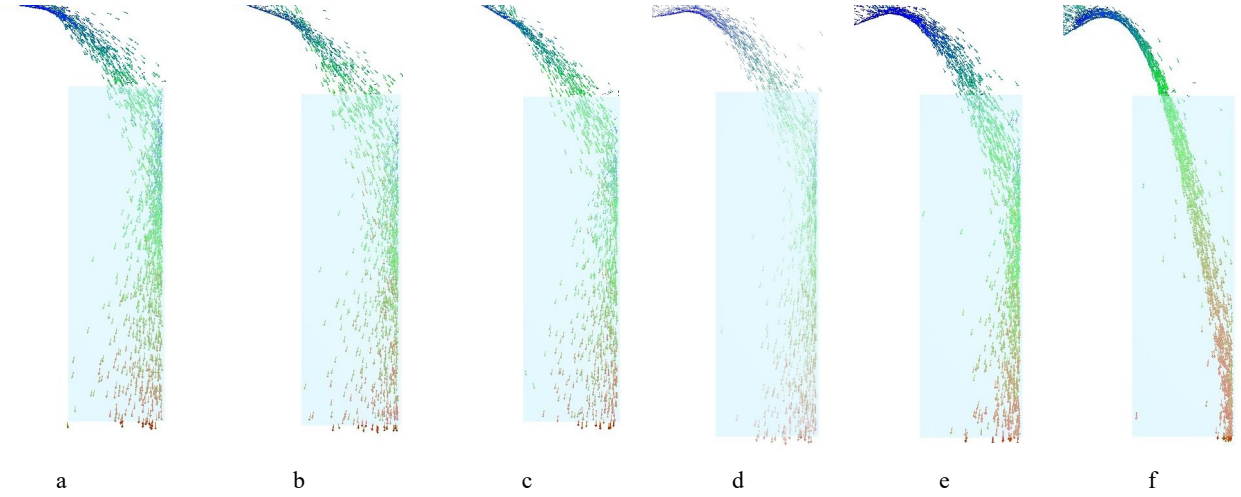


**Fig. 13.** Influence of belt angle change on particle sportswear: a – 10°; b – 20°; c – 30°; d – -10°; e – -20°; f – -30°

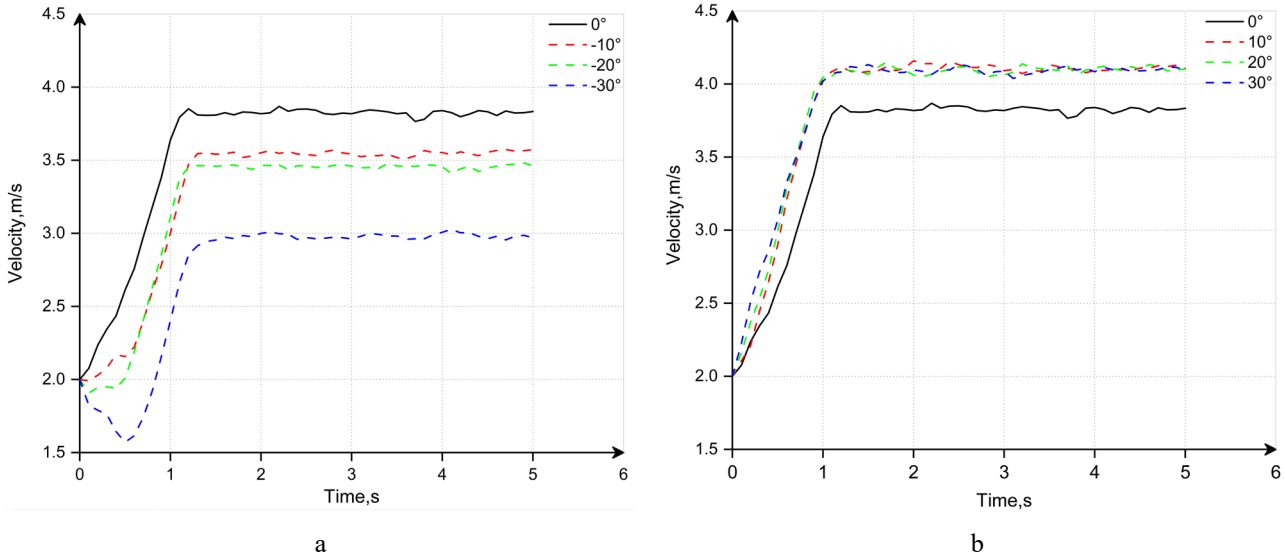


**Fig. 14.** Graph of different conveyor belt angles and particle velocity: a – angle decreases; b – angle increases

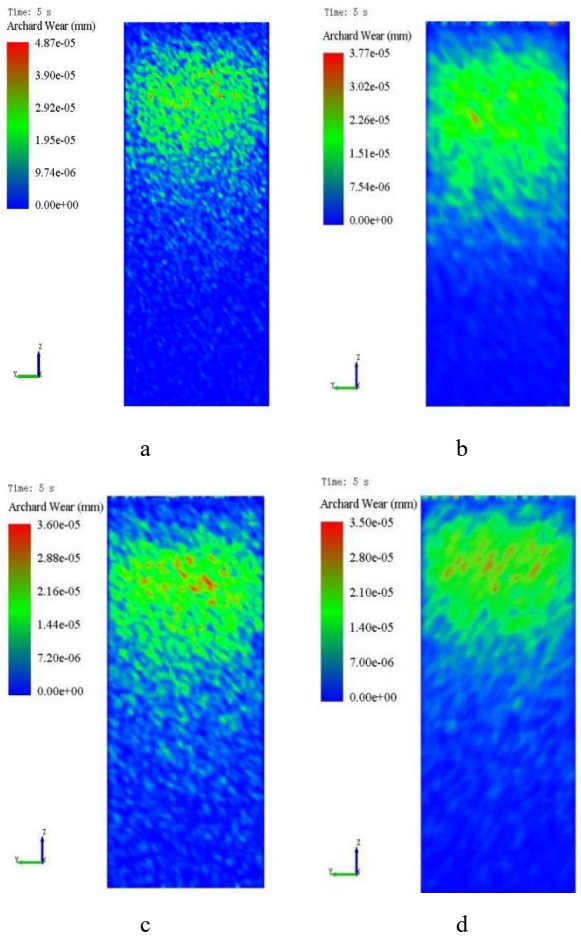


**Fig. 15.** Wear cloud map of conveyor belt 0 to 30 chute: a – 0°; b – 10°; c – 20°; d – 30°

This is different from the research method used by Thompson et al. [25], our study expands on this knowledge by measuring the impact of the conveyor belt angle on wear, a factor that has not been thoroughly investigated in existing literature. Through adjusting the conveyor belt angle, we gain valuable insights into how materials wear at different angles on the chute, contributing to a deeper understanding of discharge chute wear.

Additionally, while adjusting the speeds and angles of conveyor belts has been effective in minimizing chute wear, such alterations can also influence coal transport efficiency. Reducing the speed of the conveyor belt may result in a lower volume of coal transported per hour, thereby affecting overall transportation performance. Likewise, modifying the angle of the conveyor belt could change material flow characteristics, further influencing loading and unloading efficiency.

Consequently, when exploring strategies for wear reduction, it is crucial to assess any potential adverse effects these modifications might have on transportation efficiency. To lessen impacts on transportation efficiency during actual operations, consider implementing the following approaches.

Modify belt speeds during off-peak hours to reduce wear without significantly diminishing total transport volumes. Improve chute durability by refining its design and utilizing more abrasion-resistant materials while preserving transport efficiency. Create a regular maintenance and inspection schedule to ensure that the conveyor system functions at optimal performance levels, balancing wear reduction with efficient transportation.

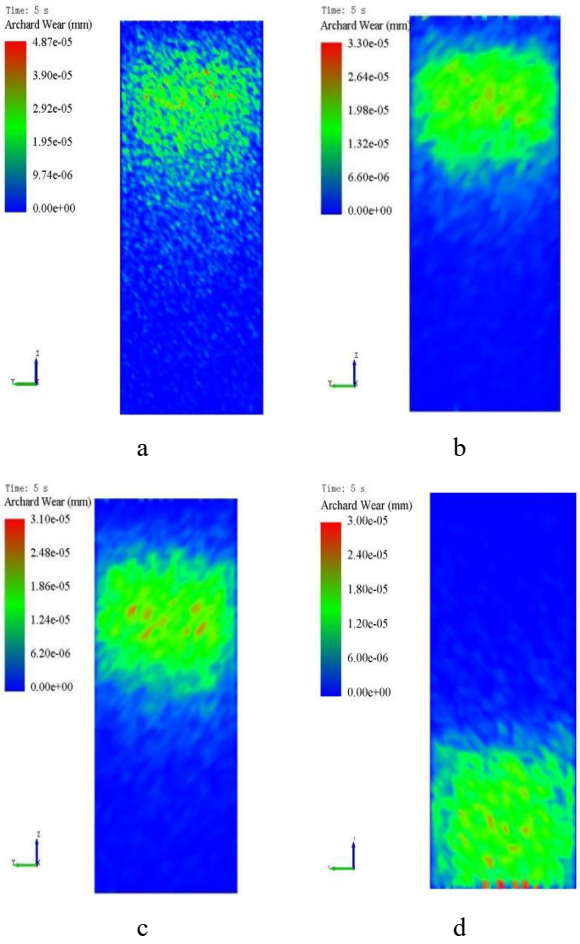


**Fig. 16.** Wear cloud diagram of conveyor belt 0 to –30 chute: a – 0°; b – -10°; c – -20°; d – -30°

## 5. CONCLUSIONS

The objective of this study is to examine the issue of wear in a chute that is exposed to particles. Through the utilization of numerical simulation and quantitative analysis techniques, the research aims to explore the patterns of wear in the chute caused by variations in particle velocity and conveyor belt angle.

1. When the speed of the conveyor belt is gradually reduced under similar circumstances, there is a decrease in particle velocity, leading to diminished wear on the chute. The primary form of wear on the chute due to particle impact is tangential.
2. While maintaining all other variables constant, making gradual alterations to the angle of the conveyor belt leads to a decrease in chute wear. An increase in the clockwise angle results in reduced chute wear; however, as particle velocity increases, there is a point at which chute wear plateaus. Conversely, an increase in counterclockwise angle leads to a reduction in particle velocity and subsequently results in a gradual decrease of chute wear.

In conclusion, to minimize the wear resulting from material impact on the chute, it is recommended to adjust the angle of the conveyor belt and regulate the speed of material transfer. Optimal measures involve limiting counterclockwise rotation within the natural rest angle of materials and implementing controlled clockwise rotation. The prioritization of conveyor belt speed management should focus on enhancing material transport efficiency while seeking opportunities to reduce material transfer velocity when feasible. These actions can improve material distribution and mitigate wear caused by impact.

This research not only enhances theoretical understanding but also carries significant practical relevance. By refining the operational parameters of conveyor belts, we can markedly boost both the efficiency and safety of coal transport systems. Nonetheless, this study has certain constraints, such as discrepancies between simulated settings and actual conditions, along with a necessity for further validation of the wear prediction model. Future research could delve into various aspects: investigating new materials and design approaches to improve wear resistance and prolong the lifespan of chutes; evaluating how environmental factors like humidity and temperature influence wear characteristics, alongside strategies to adjust operating parameters accordingly. In conclusion, this study offers an innovative viewpoint on managing chute wear in coal transportation systems, which is crucial for enhancing transport efficiency and reducing maintenance expenses.

## *Acknowledgments*

The authors wish to convey their profound appreciation to the following individuals and institutions for their backing and assistance during the course of this study. Firstly, we are indebted to Zhonglian Runshi Xinjiang Coal Industrial Co., Ltd. for furnishing us with the data, which is of vital significance for our simulation and validation research.vWe sincerely acknowledge all the graduate students and technical personnel involved in this study, who have made significant contributions to the experimental design, data collection, and analysis. We firmly believe that the completion of this study would not have been feasible without the support and assistance of these individuals and institutions. We extend our deepest respect and gratitude for their generous support and valuable time.

**REFERENCES**

1. **Xie, J.C., Yang, Z.J., Wang, X.W., Wang, S.P., Zhang, Q.** A Joint Positioning and Attitude Solving Method for Shearer and Scraper Conveyor under Complex Conditions *Mathematical Problems in Engineering* 2017: pp. 14. https://doi.org/10.1155/2017/3793412
2. **Panigrahi, S., Praharaj, S., Basu, S., Ghosh, S.K., Jaha, S., Pande, S., Vo-Dinh, T., Jiang, H., Pal, T.** Self-assembly of Silver Nanoparticles: Synthesis, Stabilization, Optical Properties, and Application in Surface-enhanced Raman Scattering *The Journal of Physical Chemistry B* 110 (27) 2006: pp. 13436 – 13444. https://doi.org/10.1021/jp062119l
3. **Hao, S.Q., Wang, S.B., Malekian, R., Zhang, B.Y., Liu, W., Li, Z.** A Geometry Surveying Model and Instrument of a Scraper Conveyor in Unmanned Longwall Mining Faces *IEEE Access* 5 2017: pp. 4095 – 4103 https://doi.org/10.1109/ACCESS.2017.2681201
4. **Chen, H., Wang, R.** Study on Wear of Scraper Conveyor Chute *International Conference on Interaction Sciences* 2015: pp. 2254 – 2257. https://api.semanticscholar.org/CorpusID:135600295
5. **Wang, S.P., Yang, Z.** Improve Design and Analysis on Transitional Chute of Scraper Conveyor *Advanced Materials Research* 145 2010: pp. 541 – 545. https://api.semanticscholar.org/CorpusID:137546672
6. **Hutchings, I., Shipway, P.** 5 - Sliding wear, in: I. Hutchings, P. Shipway (Eds.) Tribology (Second Edition), *Butterworth-Heinemann* 2017: pp. 107 – 164. https://api.semanticscholar.org/CorpusID:136271209
7. **Moore, M.A.** Abrasive Wear *International Journal of Materials in Engineering Applications* 1 (2) 1978: pp. 97 – 111. https://doi.org/10.1016/S0141-5530(78)90054-7
8. **Piazzetta, G.R., Lagoeiro, L.E., Figueira, I.F.R., Rabelo, M.A.G., Pintaude, G.** Identification of Abrasion Regimes Based on Mechanisms of Wear on the Steel Stylus used in the Cerchar Abrasiveness Test *Wear* 2018: pp. 181 – 189. https://doi.org/10.1016/j.wear.2018.07.009
9. **Benincá, F.P., Romero, M.C., Camporez, R.M., Neto, C.A.R., Strey, N.F., Scandian, C.** Evolution of Morphology, Microstructure and Hardness of Bodies and Debris during Sliding Sear of Carbon Steels in a Closed Tribosystem *Wear* 2023: pp.523 https://doi.org/10.1016/j.wear.2023.204809
10. **Bialobrzeska, B., Kostencki, P.** Abrasive Wear Characteristics of Selected Low-alloy Boron Steels as Measured in both field Experiments and Laboratory Tests *Wear* 2015: pp. 149 – 159. https://doi.org/10.1016/j.wear.2015.02.003
11. **Nahvi, S.M., Shipway, P.H., McCartney, D.G.** Particle Motion and Modes of Wear in the Dry Sand-rubber Wheel Abrasion Test *Wear* 2009: pp. 2083 – 2091. https://doi.org/10.1016/j.wear.2009.08.013
12. **Xu, L., Wei, S., Xiao, F., Zhou, H., Zhang, G., Li, J.** Effects of Carbides on Abrasive Wear Properties and Failure Behaviours of High Speed Steels with Different alloy Element Content *Wear* 2017: pp. 968 – 974. https://doi.org/10.1016/j.wear.2017.01.021
13. **Woldman, M., Heide, E.V., Schipper, D.J., Tinga, T., Masen, M.A.** Investigating the Influence of Sand Particle Properties on Abrasive Wear Behaviour *Wear* 2012: pp. 419 – 426. https://doi.org/10.1016/j.wear.2012.07.017
14. **Shi, Z., Zhu, Z.** Case Study: Wear Analysis of the Middle Plate of a Heavy-load Scraper Conveyor Chute under a Range of Operating Conditions *Wear* 2017: pp. 36 – 41. https://doi.org/10.1016/j.wear.2017.03.005
15. **Rotter, J.M., Holst, J.M.F.G., Ooi, J.Y., Sanad, A.M.** Silo Pressure Predictions Using Discrete–element and Finite–Element Analyses *Philosophical Transactions of the Royal Society of London. Series A: Mathematical, Physical and Engineering Sciences* 1998: pp. 2685 – 2712. https://doi.org/10.1098/rsta.1998.0293
16. **Grima, A.P., Wypych, P.W.** Discrete Element Simulation Validation: Impact Plate Transfer Station, 2010. https://api.semanticscholar.org/CorpusID:54865711

17. **Hastie, D.B., Wypych, P.W., David, H., Wypych, P.W.** Experimental Validation of Particle Flow through Conveyor Transfer Hoods Via Continuum and Discrete Element Methods *Mechanics of Materials* 2010: pp. 383 – 394. https://doi.org/10.1016/j.mechmat.2009.11.007
18. **Jafari, A., Nezhad, V.S.** Employing DEM to Study the Impact of Different Parameters on the Screening Efficiency and Mesh Wear *Powder Technology* 2016: pp. 126 – 143. https://doi.org/10.1016/j.powtec.2016.04.008
19. **Chen, G.M. Schott, D.L., Lodewijks, G.** Sensitivity Analysis of DEM Prediction for Sliding Wear by Single Iron Ore Particle *Engineering Computations* 2017: pp. 2031 – 2053. https://doi.org/10.1108/EC-07-2016-0265
20. **Zhou, L., Li, T., Liu, Z., Ma, H., Xu, C., Dong, Y., Zhao, Y.** An Impact Energy Erosion Model with an Energy Allocation Rule for the Discrete Element Method *Wear* 2024: pp. 540 – 541. https://doi.org/10.1016/j.wear.2023.205233
21. **Hoomans, B.P.B., Kuipers, J.A.M., Briels, W.J., Swaaij, W.P.M.** Discrete Particle Simulation of Bubble and Slug Formation in a Two-dimensional Gas-fluidised bed: A Hard-sphere Approach *Chemical Engineering Science* 1996: pp. 99 – 118. https://doi.org/10.1016/0009-2509(95)00271-5
22. **Jankowski, R.** Non-linear Viscoelastic Modelling of Earthquake-induced Structural Pounding *Earthquake Engineering & Structural Dynamics* 2005: pp. 595 – 611. https://doi.org/10.1002/eqe.434
23. **Zhang, Y.Q., Li, X.H., Ren, J.J., Tan,B.** Wear Analysis on Bucket Tooth of WK-75 Mining Excavator *Chinese Journal of Engineering Design* 2015: pp: 493 – 498. https://doi.org/10.3785/j.issn.1006-754X.2015.05.014
24. **Zhang, H., Ding, H.H., Cui, X.L., Wang, Y., Han, Z.Y., Meli, E., Wang, W.J.** Experimental Investigation on the Effect of Contact Forces on Uneven Longitudinal Wear of Rail Material *Wear* 2023: pp. 532 – 533. https://doi.org/10.1016/j.wear.2023.205108
25. **Thompson, J.A., Berry, L., Southern, S., Walls, W.K., Holmes, M.A., Brown, S.G.R.** The Effect of Mesh Discretisation on Damage and Wear Predictions using the Discrete Element Method *Applied Mathematical Modelling* 2022: pp. 690 – 710. https://doi.org/10.1016/j.apm.2022.01.005